Impact of Separation Distance on Multi-Vane Radiometer Configurations

B. M. Cornella[a], A. D. Ketsdever[a], N. E. Gimelshein[b], and S. F. Gimelshein[b]

[a]*University of Colorado at Colorado Springs, Department of Mechanical and Aerospace Engineering, Colorado Springs, CO 80918*
[b]*ERC, Inc. Edwards AFB, CA 93524*

Abstract. The radiometric force produced by a linear array of three radiometer vanes has been assessed numerically using an argon carrier gas and experimentally using air. The separation distance between the three vanes of the array was varied between 0 and 120 percent based on the height of an individual radiometer vane of 40mm. Qualitative agreement between the numerical and experimental results is shown as a function of operating Knudsen number, vane separation distance, and surrounding chamber geometry. Both sets of results indicate an asymptotic trend in maximum force as the separation distance increases as well as a shift in the maximum force Knudsen number. Small chamber effects for both numerical and experimental results indicate an increase of the total force ranging from a factor of 2.5 to 4. Quantitatively, however, the numerical simulations yield forces approximately an order of magnitude higher than observed in the experiments due to differences in carrier gas and accommodation coefficient as well as the two dimensional nature of the numerical simulations versus the three dimensional experiment.

Keywords: radiometer, radiometric force, ES-BGK equation.
PACS: 51.10.+y

INTRODUCTION

A radiometer consists of a relatively thin vane with a thermal gradient imposed between its two sides. In the rarefied flow regime, the thermal gradient exerts a force on the vane that tends to move the vane from the hot to the cold side. There are generally three major components to the force: (1) a pressure difference between the gas on the hot and cold sides (pressure force), (2) a force near the edge of the vane caused by non-uniform gas heating (edge force), and (3) a shear force due to thermal creep along the thickness of the vane (shear force). Molecules that impact the hot side have higher average velocities than those that strike the cold side; therefore, the direction of the pressure force is from hot to cold. In general, the shear force acts in the direction of cold to hot or in the opposite direction of the pressure force. Thus, the net force acting on the radiometer vane is a balance between the pressure and edge forces and the shear.

The relative contributions of these forces vary with vane geometry and operating conditions. For example, in nearly free molecular flow, the pressure force dominates where a lack of inter-molecular collisions allows a pressure difference to be set up in the flow between the hot and cold sides. However as the operating pressure is increased, the hot and cold side pressures are able to equilibrate through collisions, and the edge effect can be the dominate force production mechanism. For geometries where the thickness is relatively large compared to the other dimensions of the vane, the shear force can be an important factor. The shear force is also a major component of the net force at higher operating pressures (i.e. pressures higher than those where the maximum net force is observed). A comprehensive review of radiometric forces is given in these proceedings by Gimelshein et al.[1] In order to maximize the force production from a given geometry of radiometer vanes, the relative contribution to the net force of all three force production mechanisms must be fully understood.

Recently, radiometric forces have shown promise for applications as diverse as atomic force microscopy[2] to near-space propulsion.[3] Both of these seemingly different applications require high force density (i.e. N/m^2) to be effective. A previous numerical study[4] has shown that arrays of multiple radiometer vanes, operating in relatively close proximity, produce a much higher force per unit area than the same number of vanes working independently.

This research seeks to experimentally verify the numerical results and suggest techniques for optimizing the force production from an array of radiometer vanes. The effect of vane separation distance on the net force produced by a multi-vane array is quantified.

NUMERICAL APPROACH

A finite volume solver SMOKE[5] has been used to deterministically solve the ellipsoidal statistical kinetic equation.[6] SMOKE is a parallel code based on conservative numerical schemes developed by Mieussens.[7] The code can provide solutions for both two-dimensional and axisymmetric flows. A second order, spatial discretization was used with implicit time integration. Fully diffuse reflection with complete energy accommodation was applied at all radiometer and surrounding chamber surfaces. The lower boundary was set as the symmetry plane. Three radiometer vanes in a linear array were studied at various separation distances. The height of the radiometer vane was taken to be 40mm, and the vane thickness was set at 3.4 mm. For the 2-D simulations, the length dimension for the radiometer vanes was infinite. The temperature of the hot side of the radiometer vane was set to 403 K and the cold side was set to 382 K. Argon was used as the working gas at pressures ranging from 0.5 to 1.4 Pa. Two sets of simulations were run. The first set was run for a surrounding chamber with dimensions of 2 m by 0.5 m thick with the chamber walls at a set temperature of 300 K. The second set of simulations was run for a small surrounding chamber with dimensions of 32 cm by 16 cm thick. To simulate the experimental conditions, the chamber wall temperature directly opposite the heated radiometer vane was set to 314 K and all other chamber walls were set to 306 K.

Grid convergence was achieved by increasing the number of spatial nodes and points in velocity space. The latter was (25,25,15) for the results presented in this study. The number of spatial cells varied from 60,000 to 100,000 depending on the size of the surrounding chamber. The temporal convergence was also controlled, and the total error in the force calculations was estimated to be less than one percent in all cases.

EXPERIMENTAL SET UP

The experimental set up is shown schematically in Fig. 1. An array of three radiometer vanes was placed in a stainless steel vacuum chamber with a diameter of 1m and length of 2 m. The vacuum chamber is initially pumped to the 10^{-6} Torr level with a 3500 L/s turbomolecular pump. Gas is introduced into the chamber and a constant chamber pressure is maintained with a minimum flow rate by reducing the pumping area with a pendulum gate valve. The chamber pressure, measured by a high precision baratron, was varied from 0.5 to 2.0 Torr. Air was used as the working fluid in the experiments.

The radiometer vanes used in this study were each commercially available Peltier coolers operating on the thermoelectric effect. A potential supplied to the Peltier device produces a temperature difference between to ceramic plates. The radiometer vanes were 40 mm square with a thickness of 3.4 mm. Two experimental configurations were tested. The first test was for the surrounding chamber as the stainless steel vacuum chamber (1 m diameter by 2 m long). In this configuration, the radiometer vane temperature difference was chosen to be 25 K with a hot side temperature of 403 K and a cold side temperature of 378 K. In the second experimental configuration, a small surrounding chamber with dimensions of 32 cm by 16 cm by 12 cm thick was used as shown in Fig. 1. The temperature at various locations on the small chamber was monitored by thermocouples. In this configuration, the radiometer vane temperature difference was also chosen to be 25 K with a hot side temperature of 431 K and a cold side temperature of 406 K. The overall temperature increase on the radiometer sub-vanes is attributed to the proximity of the small chamber walls to the vanes. However, the temperature difference between the hot and cold surfaces of the vane remained approximately the same for both the large and small chamber configurations. During the experiment, the temperature on the small chamber surface directly opposite the hot radiometer vane surface was measured as 314 K while the remaining surfaces of the small chamber were measured as 306 K. These temperatures along with the temperature of the radiometer vanes were found to be relatively independent of chamber pressure over the range used in this study.

The spacing between the three radiometer vanes was varied to assess the performance of the array as a function of the vane separation distance. The vane separation (δ) was measured as a ratio of the separation distance to vane height (40 mm) and was varied between 0 and 1.2 in the experiment. To assess the performance of the array, the three radiometer vanes were attached to a modified nano-Newton Thrust Stand (nNTS) which accurately measured the force produced by the array. Details of the nNTS and its calibration system can be found Selden and Ketsdever.[8] The nNTS had a measurement standard deviation below one percent and a resolution of 400 nN.

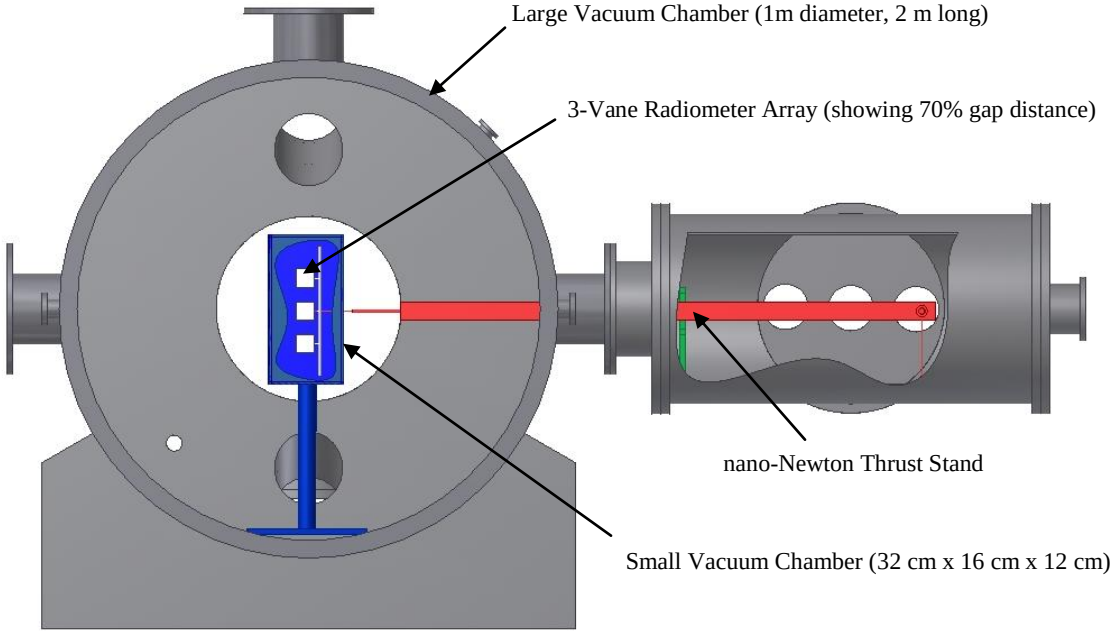

FIGURE 1. Radiometer vane array experimental set up.

RESULTS AND DISCUSSION

Numerical Simulations

Numerical results of the radiometric force produced in the large surrounding chamber are shown in Fig. 2(a) as a function of chamber pressure and vane separation distance. Results for the small chamber are shown in Fig. 2(b). As expected, the total force is larger in the small chamber due to the effects of the chamber wall proximity. A similar influence of the chamber walls was observed in previous research.[9] The pressure at which the maximum force occurs changes with the separation distance due to the changing characteristic length of the device. For example with $\delta = 0$ for the large chamber, the characteristic length is the length of all three sub-vanes. For $\delta = 0.4$, the characteristic length includes the length of all three sub-vanes and some fraction of the spacing between the vanes (i.e. the characteristic length has increased). In general, the maximum force occurs for a Knudsen number of approximately 0.03; therefore, as δ increases, the maximum force occurs at correspondingly higher operating pressures.

Figure 3(a) shows a direct comparison between the small and large chamber configurations as a function of pressure for $\delta = 0.8$. The small chamber data uses the experimentally determined wall temperatures described in the previous section. The radiometric force produced in the small chamber configuration is larger than the large chamber configuration by a factor of 2.5 to 4 times (depending on the pressure). Figure 3(b) shows the total force produced in the small chamber for two chamber wall temperatures at a fixed pressure of 1.1 Pa. The experimentally determined wall temperatures (see previous section) produce a higher net force than a fixed wall temperature of 300 K. The percent difference ranges from 8.4% at $\delta = 0$ to 6.4% at $\delta = 1.2$. The majority of the difference in the small chamber data as a function of chamber wall temperature can be attributed to a higher momentum from the molecules impacting the vane that originate from the higher temperature chamber wall.

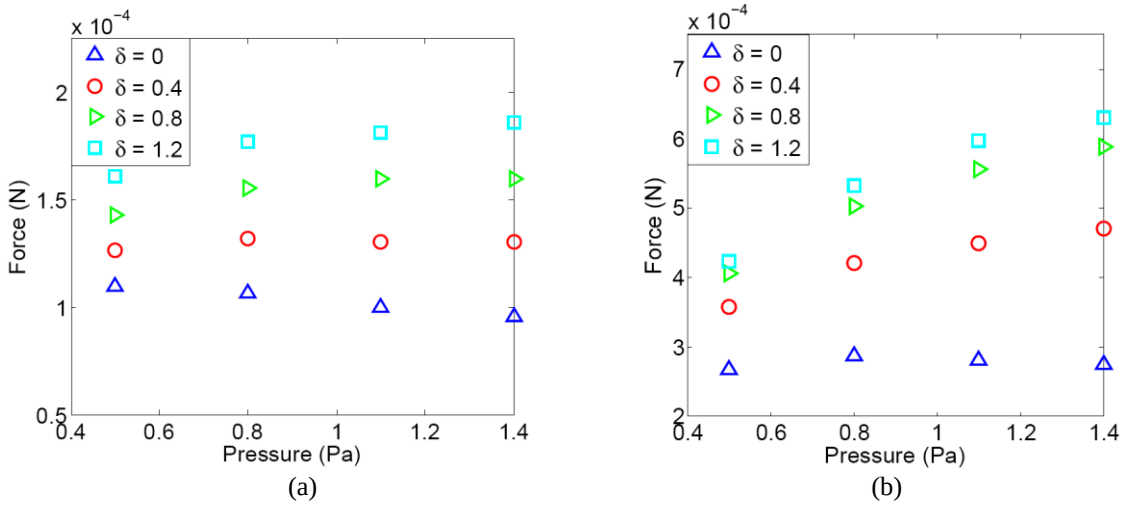

FIGURE 2. Numerical results for total radiometric force as a function of pressure and separation distance for (a) the small chamber configuration and (b) the large chamber configuration.

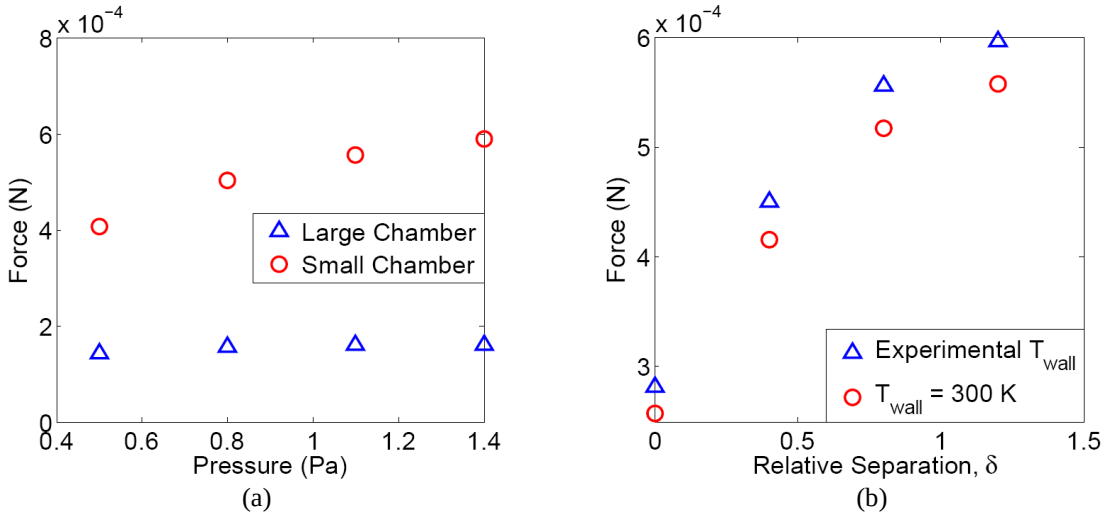

FIGURE 3. Numerical results for total radiometric force for (a) small and large chamber configurations as a function of pressure for δ=0.8 and (b) small chamber configuration as a function of separation distance for two different chamber wall temperatures.

Experiments

Experiments were performed with air as the working gas. Figure 4(a) shows the radiometric force produced by the three vane radiometer as a function of operating pressure for various values of the vane separation, δ. The statistical error in the experimental data (±σ) contained in Fig. 4 is less than the symbol size and, therefore, is not shown. The data in Fig. 4 was taken in the large vacuum chamber configuration. With δ = 0, the three vane radiometer acts as a single vane with dimensions 120 mm high by 40 mm wide. By separating the vanes, the overall perimeter of the device increased by 50%, increasing the contribution of the edge force produced by the radiometer. The maximum force shifts to higher pressures as the vane separation distance increases due to a change in the overall device's effective characteristic length. Figure 4(b) shows the maximum force produced as a function of δ. The maximum force asymptotes to approximately 22.2 μN. At δ = 0.7 the force produced is approximately 96% of the maximum achievable force while only increasing the overall length of the radiometer by 48% over the single vane.

Figure 5 shows the difference in force produced between the large and small chamber configurations. Again, the error in this set of data is less than the symbol size in the figure and therefore is not shown. Over all values of δ, the radiometer in the small chamber produced approximately 2.5 times higher force than the same radiometer configuration in the large chamber. The force produced by a given radiometer geometry is strongly influenced by

the proximity to the surrounding chamber walls. The maximum force produced by the device in the small chamber asymptotes to approximately 51.3 μN. As was the case in the large chamber configuration, the force produced at δ = 0.7 is approximately 96% of the asymptotic value indicating that the general trend for the maximum produced force versus vane separation is independent of chamber wall proximity. Therefore, only the overall force production is affected by the small chamber.

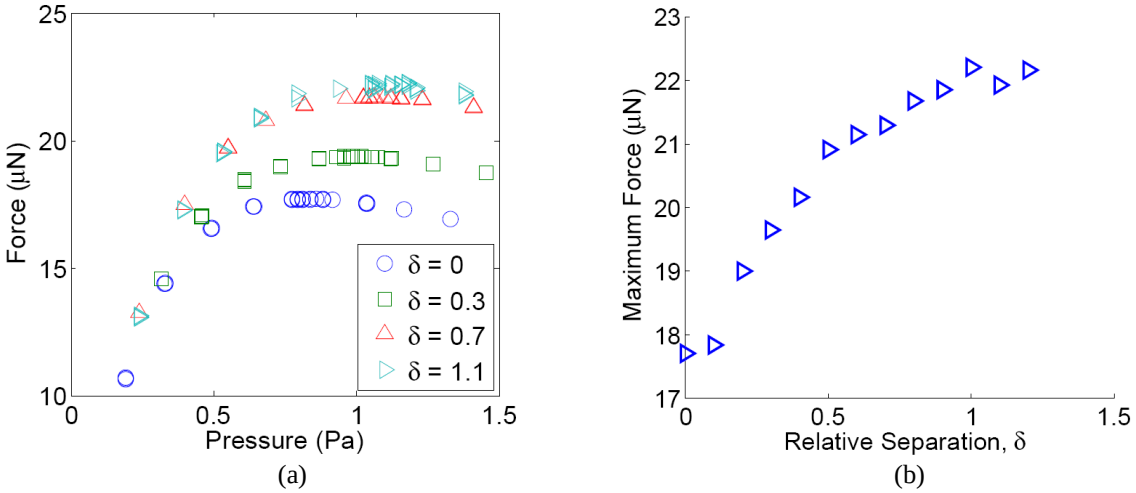

(a) (b)

FIGURE 4. Experimental results for total radiometric force (a) Force as a function of pressure and separation distance and (b) maximum force as a function of separation.

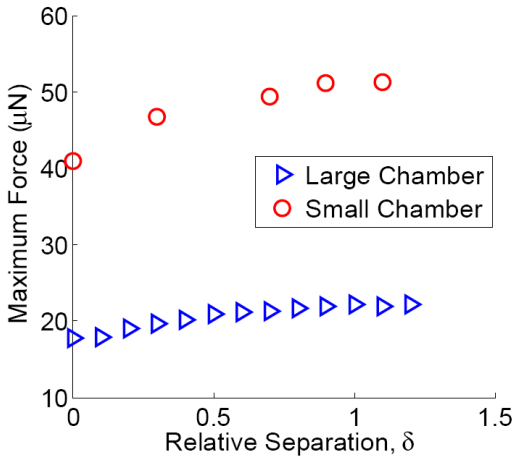

FIGURE 5. Maximum force as a function of separation for large and small chamber configurations.

Discussion

Qualitatively, the results for the numerical simulations and experimental data are generally very similar. As shown in Fig. 2, the numeric results show an increase in force with increasing δ whereby the maximum force asymptotes to some value. Likewise, the experiments showed the same asymptotic trend as δ increases. In both the experimental and numerical studies, the pressure at maximum force increases with increasing gap distance and decreasing wall proximity (due to the change in overall system characteristic length).

Quantitatively, however, there are a few discrepancies between numerical and experimental results. On average, the resulting force from the numerical data is roughly an order of magnitude higher than the experiment. Also, despite the fact that the pressure at which maximum force occurs is consistent between the two analyses on average (accounting for the change in carrier gas), the variation is more pronounced in the numerical study. These discrepancies can largely be attributed to the difference in carrier gas, the accommodation coefficient used in the numerical simulations, and the three-dimensional nature of the experiment. The experiments were performed with air as the working gas, whereas the numerical simulations used argon. Selden[10] shows both numerically and

experimentally that there is approximately a 10% difference in the force production between argon and air at similar pressures with argon producing a higher force. Although air should produce a higher force because of its lower average molecular weight, the difference can be credited to the internal energy modes for air. All numerical simulations used an accommodation coefficient, a_c, of 1 for pure argon. Previous studies indicate that the accommodation coefficient for argon is between 0.85 and 0.96 depending on the interacting surface.[11] Finally, the comparison between a two-dimensional simulation and three-dimensional experiment also contributes to the differences between the numerical and experimental data. Future work is needed to investigate the influence of the third dimension to accurately model radiometric flows. Although these corrections do not completely account for the discrepancies between data sets, the differences between the numerical and experimental analysis is presumably reduced to with an order of magnitude.

CONCLUSIONS

This study sought to investigate the impact of vane separation in multi-vane radiometers while comparing numerical simulations to experimental data. In general, the numerical and experimental results show qualitative agreement. Both sets of data show an asymptotic trend in maximum produced force as the relative vane separation, δ, increases. The data indicates that there exists a range of separation distances which produce a high percentage of the maximum value (at $\delta = \infty$) without dramatically increasing the overall length of the device. For instance, according to experimental data, at $\delta = 0.7$, the force produced by the multi-vane is 96% of the asymptotic value while only increasing the overall length by 48% of a single vane. Both numerical and experimental results also show a significant increase in force with a smaller chamber setup. The numerical simulations showed an increase factor from 2.5 to 4 while the experiments indicated a similar factor of 2.5. These results verify previous studies on the effects of chamber wall proximity.[9] Qualitative changes in the pressure at which maximum force occurs with δ and chamber wall proximity are also consistent between experimental and numerical data. As δ increase or the surrounding chamber become smaller, the pressure at maximum force production increases due the changes in characteristic length associated with the overall system.

ACKNOWLEDGMENTS

The authors wish to thank the United States Air Force Research Laboratory, Propulsion Directorate (Edwards AFB, California) for their support of this research. The data taking skills of Mr. Chris Flatley and the figure making skills of Ms. Joelle Suits are greatly appreciated.

REFERENCES

1. S. Gimelshein, N. Gimelshein, A. Ketsdever, and N. Selden. In *Proceedings of the 27th International Symposium on Rarefied Gas Dynamics*, edited by AAAA, AIP Conference Proceedings NNNN, American Institute of Physics, Melville, NY, 2011, pp. PPP-PPP.
2. A. Passian, A. Wig, F. Meriaudeau, T. Ferrell, and T. Thundat. *J. Appl. Phys*, **92**, 6326-6333 (2002).
3. B. Cornella, A. Ketsdever, S. Gimelshein and N. Gimelshein. *AIAA paper 2010-4516*, 10th Joint Thermophysics and Heat Transfer Conference, Chicago, IL (2010).
4. N. Gimelshein, S. Gimelshein, A. Ketsdever, and N. Selden. *J. MEMS*, submitted (2010).
5. D. Wadsworth, N. Gimelshein, S. Gimelshein, and I. Wysong. In *Proceedings of the 26th International Symposium on Rarefied Gas Dynamics*, edited by T. Abe, AIP Conference Proceedings 1084, American Institute of Physics, Melville, NY, 2008, pp. 206-211.
6. L. Holway. *Proceedings of the 4th International Symposium on Rarefied Gas Dynamics*, edited by J. De Leeuw, Academic Press, NY, 1966, pp. 193-215.
7. L. Mieussens. *J. Comp. Phys*, **162**, 429-466 (2000).
8. N. Selden and A. Ketsdever, *Rev. Sci. Instrum*., **74**, 5249-5254 (2003).
9. N. Selden, S. Gimelshein, N. Gimelshein, A. Ketsdever. In *Proceedings of the 26th International Symposium on Rarefied Gas Dynamics*, ed. T. Abe, AIP Conference Proceedings 1084, American Institute of Physics, Melville, NY, 2009, pp. 1009-1014.
10. N. Selden, "Experimental Study of Radiometric Forces with Comparison to Computational Results", Ph.D. Thesis, University of Southern California, 2009.
11. W. M. Trott, D. J. Rader, J. N. Castañeda, J. R. Torczynski, and M. A. Gallis, "Measurement of gas-surface accommodation," *Proceedings of the 26th International Symposium on Rarefied Gas Dynamics*, Kyoto, Japan, July 2008.